PHYSICAL REVIEW C **86**, 041301(R) (2012)

Influence of the *np* interaction on the β decay of ^{94}Pd

B. S. Nara Singh,[1] T. S. Brock,[1] R. Wadsworth,[1] H. Grawe,[2] P. Boutachkov,[2] N. Braun,[3] A. Blazhev,[3] Z. Liu,[4] M. Górska,[2] S. Pietri,[2] D. Rudolph,[5] C. Domingo-Pardo,[2] S. J. Steer,[6] A. Ataç,[7] L. Bettermann,[3] L. Cáceres,[2] T. Engert,[2] T. Faestermann,[8] F. Farinon,[2] F. Finke,[3] K. Geibel,[3] J. Gerl,[2] R. Gernhäuser,[8] N. Goel,[2] A. Gottardo,[4] J. Grębosz,[9] C. Hinke,[8] R. Hoischen,[2,5] G. Ilie,[3] H. Iwasaki,[3] J. Jolie,[3] A. Kaşkaş,[7] I. Kojouharov,[2] R. Krücken,[8] N. Kurz,[2] E. Merchán,[2] C. Nociforo,[2] J. Nyberg,[10] M. Pfützner,[11] A. Prochazka,[2] Zs. Podolyák,[6] P. H. Regan,[6] P. Reiter,[3] S. Rinta-Antila,[12] C. Scholl,[3] H. Schaffner,[2] P.-A. Söderström,[10] N. Warr,[3] H. Weick,[2] H.-J. Wollersheim,[2] P. J. Woods,[4] and F. Nowacki[13]

[1]*Department of Physics, University of York, Heslington, York YO10 5DD, United Kingdom*
[2]*GSI Helmholtzzentrum für Schwerionenforschung, D-64291 Darmstadt, Germany*
[3]*IKP, Universität zu Köln, D-50937 Köln, Germany*
[4]*School of Physics and Astronomy, University of Edinburgh, EH9 3JZ Edinburgh, United Kingdom*
[5]*Department of Physics, Lund University, S-22100 Lund, Sweden*
[6]*Department of Physics, University of Surrey, Guildford GU2 7XH, United Kingdom*
[7]*Department of Physics, Ankara University, 06100 Tandoğan, Ankara, Turkey*
[8]*Physik Department E12, Technische Universität München, D-85748 Garching, Germany*
[9]*The Institute of Nuclear Physics PAN, PL-31342 Kraków, Poland*
[10]*Department of Physics and Astronomy, Uppsala University, SE-75120 Uppsala, Sweden*
[11]*Faculty of Physics, University of Warsaw, PL-00-681 Warsaw, Poland*
[12]*Department of Physics, Oliver Lodge Laboratory, University of Liverpool, L69 7ZE Liverpool, United Kingdom*
[13]*IPHC, IN2P3-CNRS et Université de Strasbourg, F-67037 Strasbourg, France*

(Received 25 July 2012; revised manuscript received 11 September 2012; published 11 October 2012)

We present results from stopped beam rare isotope spectroscopic investigations at the GSI (RISING) experiment based on the detection of γ-ray transitions following the β decay of ^{94}Pd. A comparison between the measured low-lying level scheme of ^{94}Rh and the prediction from shell-model calculations reveals the important roles of the $g_{7/2}$ and $g_{9/2}$ orbitals in explaining the structural features. The low values of the Gamow-Teller strengths $B(GT)$ can be attributed to the influence of the neutron-proton interaction, which gives rise to an increased seniority mixing for the nuclear states, thereby leading to a fragmentation of the strength to several daughter levels. These results provide further strong indications that ^{94}Pd resides in the middle of a structural transition region in the Pd isotopes as the $N = Z$ line is approached.

DOI: 10.1103/PhysRevC.86.041301 PACS number(s): 21.60.Cs, 23.20.Lv, 23.35.+g, 23.40.Hc

The phenomena exhibited by $N \sim Z$ nuclei in the region southwest of ^{100}Sn can generally be understood by considering only a few valence orbitals and are particularly dominated by the $g_{9/2}$ shell. As a result, shell-model calculations for these nuclei are feasible and the corresponding experimental data can serve as an excellent testing ground for such models [1–4]. A particularly interesting feature in this part of the nuclear landscape is the gradual demise of the $g^n_{9/2}$ seniority scheme, which is well established in the $N = 50$ isotones, as the $N = Z$ line is approached [5]. Recently, a rapid change in structure has also been observed in the case of Pd isotopes as the neutron number decreases from 50 to 46. This was interpreted in terms of an increased role of the isoscalar interaction between neutrons and protons ($T = 0$, np interaction) in $N \sim Z$ nuclei [6,7]. Indeed, ^{94}Pd was suggested to be a special case, with low-lying structural properties that are intermediate to those of its immediate even-even neighbors ^{92,96}Pd, where the lighter nucleus shows no evidence for seniority structure while the $N = 50$ isotope retains the classic seniority type level sequence [6].

A knowledge of the structure of low-lying levels and the Gamow-Teller (GT) strength distributions $B(GT)$ observed in β^+/EC decay are important elements for providing a comprehensive understanding of exotic decay modes found in nuclei close to the limits of existence. Such studies help probe the dynamics of the nucleon-nucleon interaction far from the stability line [8–10]. Indeed, the evidence for the direct two-proton decay of the 21^+ isomeric state in ^{94}Ag has been initially supported [11] and later disputed [12–14] by utilizing the data for the surrounding nuclei ^{92,94}Rh [14]. Further interest in these nuclei results from the relevance of their properties for the understanding of the astrophysical rapid-proton [15], νp [16] processes, type II supernova explosions [17] and for precision tests of the standard model [18].

In the case of ^{94}Rh, only limited low-lying structural information is available from previous works [19–22]. Two long-lived states are known with half-lives $T_{1/2} = 70.6$ (6) and 25.8 (2) s. These are henceforth referred to as ^{94m1}Rh[(4^+)] and ^{94m2}Rh[(8^+)], respectively, following the convention of Batist *et al.* [19,21]. It was established that the longer lived state was populated in the first β-decay study of ^{94}Pd [20]. The order of their excitation energies is, however, not known. Evidence for a few γ rays with energies of 558, 724, 798, 822, and 846 keV in ^{94}Rh was also found, but they could not be placed in a level scheme [20]. Batist *et al.* obtained $T_{1/2} = 9.6$ (2) s for the ground-state decay of ^{94}Pd in a total absorption spectroscopy (TAS) study [21], a result that is in good agreement with Refs. [23,24]. This work also revealed

the existence of four (1^+) states and a new (2^+) isomeric state in ^{94}Rh. The latter is referred to as ^{94m3}Rh with $T_{1/2}$ = 0.48 (3) μs and decays via a 55 keV $E2\gamma$ transition. Spin and parity assignments for these levels were based on their properties, such as half-lives, the conversion coefficients of the resulting γ rays, β-decay selection rules, and the decay data of ^{94}Rh as well as through a comparison with shell-model calculations [21].

The present work contributes to the essential data on the β decay of nuclei below the $N = 50$ shell gap and to the theoretical understanding in this region. We present a level scheme of ^{94}Rh, which is based on the detection of the individual γ transitions following the β decay of ^{94}Pd using the state-of-the-art RISING facility. A comparison between our results and shell-model calculations of level structure as well as the fragmented GT strengths indicate an increased influence of the $g_{7/2}$ orbital and the np interaction leading to mixed seniority states in this region. The previously reported two proton decay in ^{94}Ag is also briefly discussed in the context of the observed 2906-keV γ transition.

^{94}Pd nuclei were produced together with other nuclei of interest by the fragmentation of an 850 MeV/nucleon ^{124}Xe primary beam, with an intensity of 10^9 particles/s on a 4 g/cm^2 ^{9}Be target, from the SIS-18 synchrotron at the GSI Helmholtzzentrum für Schwerionenforschung laboratory, Darmstadt, Germany. Details of the setup can be found in Refs. [7,25,26]. The fragments were identified on an event-by-event basis after their separation using the fragment separator (FRS) [26–31]. Figure 1 in Ref. [25] corresponds to the data obtained from this experiment and shows a clean identification of ^{94}Pd nuclei. The ions were slowed down using an aluminium degrader at the $S4$ focal plane of the FRS, where the RISING [28–31] stopped beam setup was located. They were implanted in an "active stopper" that consisted of nine double sided silicon strip detectors (DSSSDs) arranged in three horizontal rows perpendicular to the beam direction, with three detectors in each row. Each DSSSD had 1-mm thickness, 5 × 5-cm^2 area and 16 X and 16 Y strips [32], thus allowing the location of the implantation position of the nuclei as well as the detection of the particles emitted from their subsequent decays [33]. γ rays were detected by using the 15 EUROBALL cluster detectors, each cluster comprising seven individual HPGe crystals, which were placed around the active stopper. A timing signal from a scintillator, that was placed upstream from the $S4$ focal plane, gave information about the implantation time of the nuclei (see, e.g., [28,29,34] for details). This was used to deduce the correlation time between the arrival of the nuclei of interest and their subsequent decays.

Since the experiment was not explicitly designed for the study of ^{94}Pd, the implantation profile of these nuclei in the silicon detectors was not ideal, but concentrated on the back-left DSSSD in the furthest row downstream and to the left as viewed by the beam approaching the stopper. It was found that 14 of the 16 X and all of the Y strips, totalling 224 pixels of this "active DSSSD," contained good data that were considered in our analysis. This procedure of selecting only a relevant subset of Si pixels increased the number of true spatial correlations between the implanted ^{94}Pd and their subsequent decays in the active stopper. The total implantation rate varied over the pixels, but an average value for all types of ions was ∼0.5 Hz per pixel. In other words, the time between any two consecutive implantations was $\Delta t_{\rm imp} \sim 2$ s. Therefore, the true implantation-decay correlations were only possible over a correlation time, $\Delta t_{\rm corr}$ much less than 2 s.

Figure 1 shows the prompt γ-ray spectra associated with the decay of (a) ^{94}Pd and (b) all of the nuclei implanted into the active DSSSD. It is evident from Fig. 1(a) that the 558-, 798-, 822-, 846-, 896-, 1638-, 1766-, and 2906-keV transitions are enhanced with respect to the contaminant lines. Ideally, these spectra should have been created with a correlation time much longer than the $T_{1/2} = 9.0$ s for the ground-state β decay of ^{94}Pd. Several contaminant lines are present in Fig. 1(a), because $\Delta t_{\rm corr} \sim \Delta t_{\rm imp} \sim 2$ s, while the true temporal correlations can only be expected for a $\Delta t_{\rm corr} << \Delta t_{\rm imp}$. It is worth noting that the aforementioned selection of a subset of pixels, where ^{94}Pd are mostly implanted, helps in reducing false temporal correlations with any other ions. The cleanliness of the spectra was sacrificed in the present study to gain statistics related to the relatively slow ^{94}Pd β decay. Most of the contaminant γ rays are identified as belonging to the daughter activities of ^{94}Pd, ^{95m}Pd, and ^{96}Ag nuclei, as indicated in Fig. 1.

A γ-ray spectrum was also created with the same conditions as those for Fig. 1(a), but requesting events delayed by 0.33 to 1.75 μs with respect to the β-decay signal. This time window was chosen according to the known half-life, $T_{1/2} = 0.48(3)\mu s$, of the 2^+ state in ^{94}Rh. In this spectrum, the 55-keV γ ray is observed, as expected, to be one of the prominent lines. A few contaminant lines, for example, delayed γ rays from the daughters of ^{96}Ag and ^{96}Pd, were also seen.

We obtained values for the "correlation efficiency" (CE), which is defined as the ratio between the number of counts in Figs. 1(a) and 1(b) (i.e., the γ-ray spectra associated with the decay of ^{94}Pd and all of the other nuclei, respectively) for a γ line at a given energy. These results reveal higher CE values for the γ transitions in ^{94}Rh due to their expected enhancement in Fig. 1(a). As can be seen from Fig. 1(c), the CE values for the *strong* 558-, 1766-, and 2906-keV lines are indeed similar and at least five to six times higher than the values for the contaminant lines, such as those at energies of 382, 871 (^{94}Mo), 942 (^{95}Ru), 1351/1352 (^{95}Rh/^{95}Ru), 1415 (^{96}Pd), and 1431 (^{94}Ru) keV [35]. It should be noted that for some of the other candidate lines [shown in red in Figs. 1(a) and 1(c)], somewhat smaller enhancement is seen, which could be attributed to the uncertainties resulting from the lower statistics. Furthermore, similar structures for the implantations per strip ("hit distributions") corresponding to the 558-, 1766-, and 2906-keV lines can be seen in Fig. 1(d). These distributions differ from those for the representative 1351/1352 (^{95}Rh/^{95}Ru) and 1415 keV (^{96}Pd) contaminant lines.

After a careful inspection of the data for all of the nuclei that have been produced in our experiment, we found that the 2906-keV transition could only result from the decay of either ^{94}Pd or ^{95}Pd, for which β-delayed nuclear level schemes are not known. Q-value considerations imply that the 2906-keV γ ray could originate from the decay of either ^{94}Pd to ^{94}Rh or ^{94}Rh to ^{94}Ru. This γ ray was not observed in

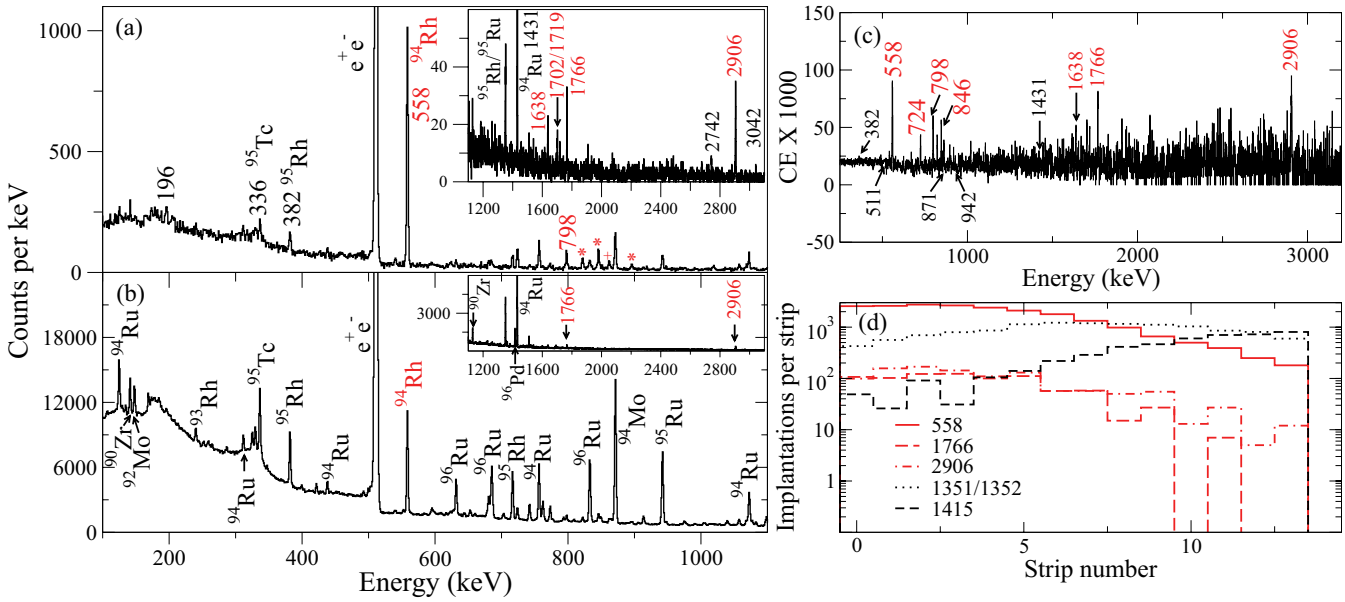

FIG. 1. (Color online) γ-ray spectra associated with the decay of (a) the ^{94}Pd nuclei, where symbols are used to mark the 822, 846, and 896 (*) and 863 keV (+) lines and (b) all of the nuclei implanted in the active DSSSD. The majority of the lines can be associated with the known decays of nuclei as indicated [35]. New as well as the known γ transitions in ^{94}Rh are marked in red (light). Unidentified peaks are marked in black (dark) only with their energies. (c) The correlation efficiencies CE (multiplied by 1000) deduced from the spectra in (a) and (b). (d) Implantations per strip in the active DSSSD (i.e., hit distributions) corresponding to several γ rays are also shown. See the text for details.

the study of the latter decay presented in Ref. [19], although several other high energy γ rays with reasonable intensity were observed, implying that the γ detection efficiency was not a limiting factor. Furthermore, evidence of a prompt-delayed coincidence, using a delay of 0.33 to 1.75 μs, between the 2906-keV γ ray and the known 55-keV transition in ^{94}Rh is found in the present work. However, this evidence is somewhat weak due to the low detection efficiency and high internal conversion coefficient for the 55-keV γ transition. These observations and the appearance of the 2906-keV line in Fig. 1(a) strongly suggest that this transition is associated with the ground-state β decay of ^{94}Pd. This is further supported by the corresponding "hit distributions" and correlation efficiencies [see Figs. 1(c) and 1(d)]. Therefore, we propose a (1^+) level in ^{94}Rh residing at 2961 keV above the 4^+ state, which decays to the 2_1^+ state by emitting a 2906-keV γ ray. This (1^+) state is likely to be the same as the (1^+) state reported in Ref. [21] residing at an energy that is 2910 (10) keV above the 4^+ state. The apparent disagreement in the energies could be due to the differences in technique used in Ref. [21]. In Figs. 1(a) and 1(c), evidence for the 1638-keV γ transition can also be found, though the signature in the CE plot is not very clear. Unfortunately, our statistics in this case do not allow us to establish a coincidence relation with any other (in particular the 55 keV) γ ray. However, noting the evidence for the (1^+) state at 1670 keV in Ref. [21] and the aforementioned fact that in our experiment the energies might be some what different, we propose a 1^+ state residing at 1693 keV that decays to the (2_1^+) state by emitting the 1638-keV γ ray.

We show the level scheme in Fig. 2 (EXP), which was deduced by utilizing our results from the above analysis and from weakly observed γ-γ coincidence relations, the spin-parity assignments from Ref. [21], and shell model calculations (see below) . All of the γ rays are placed in the level scheme. Good agreement is found between the current results for ^{94}Rh and those from Ref. [21] except for differences

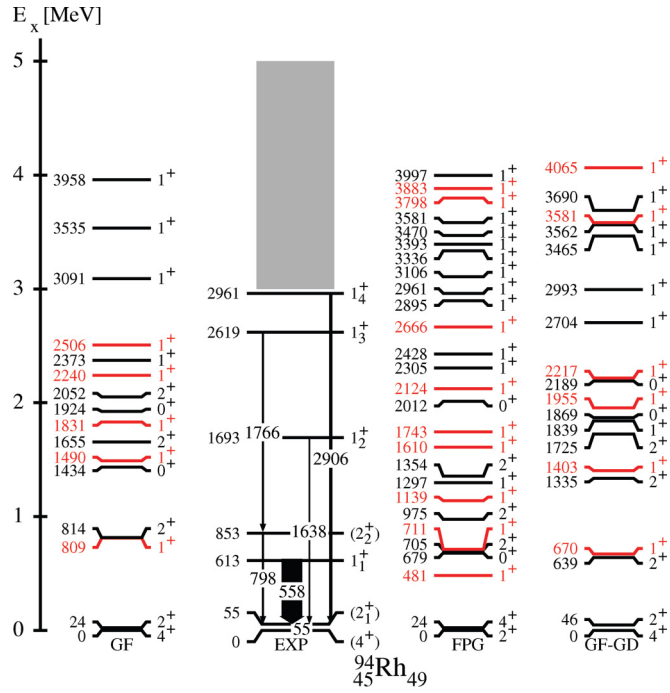

FIG. 2. (Color online) Deduced (EXP) and calculated (GF, FPG, GF-GD) level schemes for ^{94}Rh. Levels up to 4 MeV relevant for the β^+/EC decay are shown. The lowest two states in EXP correspond to ^{94m1}Rh and ^{94m3}Rh. See the text for details.

in the excitation energies of the levels residing at 1693 [1_1^+], 2619 [1_2^+], and 2961 [1_3^+] keV. As given, we propose that the 1766-keV transition originates from the 2619-keV [1_3^+] level that may well be the same as the (1^+) state at 2630 (10) keV in Ref. [21]. We also assign a level residing at 853 keV to be the (2_2^+) state, based on the coincidences seen between the 798- and 1766-keV γ rays and the energy levels (see below) found in our calculations. Additional 863-1702-keV and 822-846-896-keV mutual (but somewhat weaker) coincidences were also found from this analysis; however, we have not been able to place these in the level scheme with certainty. Therefore, they have been left out. As in the case of the 798-1766 keV sequence, these cascades have a sum energy of ~2564 keV and can originate from the level residing at 2619 keV, populating the 2^+ level at 55 keV. It should, however, be noted that the order of the transitions shown in Fig. 2 is only tentative from calculations and could not be fixed using our data. We would like to point out that even though the sum of 846 and 1719 keV is 2564 keV, we could not firmly establish a coincidence relation between these transitions.

Figure 2 shows shell-model calculations in three different approaches. Among these, the Gross-Frenkel (GF) calculation uses the empirical interaction by Gross-Frenkel [2,36] in the $\pi\nu(p_{1/2}, g_{9/2})$ model space that allows only the $\pi g_{9/2} \rightarrow \nu g_{9/2}$ and $\pi p_{1/2} \rightarrow \nu p_{1/2}$ transitions, while the calculation, which we refer to as FPG, also allows the $\pi p_{3/2} \rightarrow \nu p_{1/2}$, $\pi p_{3/2} \rightarrow \nu p_{3/2}$, and $\pi f_{5/2} \rightarrow \nu f_{5/2}$ transitions due to the extended space that also includes the $\pi\nu(f_{5/2}, p_{3/2})$ orbitals [25,26]. The approach, which is referred to as GF-GD, has $\pi\nu(p_{1/2}, g_{9/2})$ (GF) and $\nu(g_{7/2}, d_{5/2})$ model spaces and allows the one-particle–one-hole $\nu(p_{1/2}, g_{9/2})$ to $\nu(g_{7/2}, d_{5/2})$ excitations across the $N = 50$ shell, but blocks the $\pi\nu(f_{5/2}, p_{3/2})$ orbitals. This modification results in important contributions from the $\pi g_{9/2} \rightarrow \nu g_{7/2}$ GT transitions in addition to the aforementioned allowed transitions in the GF approach.

It should be noted that each of the three different calculations has deficiencies—for example, the level energies from the FPG approach are lower compared to the true values. This results from the incomplete correction for double counting [25]. The "core-excited" states that are expected to reside above ~3 MeV may be ~1 MeV higher in energy in the case of the GF-GD calculations due to truncation, which restricts the model space to one-particle–one-hole excitations. Nevertheless, a comparison with the data sheds light on the general features, such as the presence or absence of the γ transitions in ^{94}Rh. An estimation of the total $B_T(GT)$ strength is also possible by utilizing the calculations from all of the three approaches (see below). We would like to point out that at present it is not possible to simultaneously include all of the aforementioned important transitions and carry out completely consistent calculations.

TABLE I. Excitation energies, intensity analyzed γ rays, feeding intensities, and $B(GT)$ values for the four observed 1^+ daughter states.

E_x (keV)	E_γ (keV)	Feeding (%)	$B(GT)$
613	558	67.5 (6)	0.11 (3)
1693	1638	4.1 (6)	0.02 (1)
2619	798	18.1 (10)	0.29 (13)
2961	2906	10.3 (4)	0.27 (14)

Our calculations show that mostly the $1_n^+ \rightarrow 2_1^+ M1$ transitions are favored due to either the transition strengths or decay-energy considerations. Here, higher values for the subscript n correspond to the levels with higher excitation energies. As expected from our calculations, the γ decays between the 1^+ states, namely, the 2961 → 613 (2348 keV) and 2619 → 613 (2006 keV) transitions, do not appear in our spectra (cf. Figs. 1 and 2) due to the unfavorable branchings. On the other hand, a γ line corresponding to the 2564-keV M1 transition from the (1_3^+) state at 2619 keV to the (2_1^+) state at 55 keV may be expected but is, however, absent. The calculations indicate that this can be due to another competing decay via the intermediate 2_2^+ state, i.e., via the $1_3^+ \rightarrow 2_2^+ \rightarrow 2_1^+$ cascade (Fig. 2). This is in line with one of the cascades, with 1766- and 798-keV γ transitions, obtained from our γ-γ coincidence data analysis. In the context of observed coincidences, the high level density of $(0–2)^+$ states between 500 and 700 keV in the FPG approach is remarkable, and this could also certainly accommodate cascades, such as those mentioned previously with a sum energy of ~2564 keV. However, we refrain from a detailed evaluation of branching ratios, because of the deficiencies of various shell-model approaches and the limited statistics in our data.

Table I shows the $B(GT)$ values from our work. The sum $B(GT)$ strengths for the first four observed 1^+ states from our analysis of all the detected γ-ray intensities and from the TAS work [21] are 0.7 (2) and 0.56 (8) (in standard units; see Ref. [37]), respectively. These values are in agreement within the experimental uncertainties. In our analysis, when different decay paths are observed between two possible levels, we assumed that the population of the decaying level is proportional to the sum of the intensities corresponding to the lowest most γ rays in the decay cascades. Our value, 0.7 (2), also corresponds to the total strength $B_T(GT)$, because of the nonobservation of any additional strength. This value is ~3 times smaller than the experimentally deduced value of $B_T(GT) = 1.9$ (4) from Ref. [21]. This conflict can be traced to the pandemonium problem [38] and the unobserved weak cascades in our high-resolution study. In the TAS work, only the previously noted first four states in ^{94}Rh were resolved. Thus, in order to account for the remaining two-thirds of the GT strength, a hypothetical distribution of 1^+ states (based on a shell-model calculation and empirical interaction in the GF space [22]) was introduced above 3 MeV [21]. In Fig. 2, this is indicated by the shaded area. This indicates that this part of the TAS analysis might be subjected to systematic uncertainties due to the limitations of the models. The 1^+ states shown in red receive significant $B(GT)$ strengths. As can be seen, these results for the feeding differ significantly between the GF, FPG, and GF-GD approaches.

From our calculations and the $Q_{EC}(^{94}\text{Pd} \rightarrow {}^{94m1}\text{Rh} = 6.7$ MeV) value [21], we note that the $B(GT)$ strength $\{= 1.95(5) - 0.56(8) = 1.39(9)$, which is calculated using the $B(GT)$ values from the TAS work [21]$\}$ could be distributed over a few 1^+ states above 3 MeV and, therefore, is somewhat

fragmented. This would imply low intensities for the γ transitions resulting from the decay of these states. We believe that we did not observe the fragmented GT strength of 1.39(9), because of the limited γ-ray detection efficiency of our setup. This negative result strongly endorses a fragmentation of the $B(GT)$ strength, which could be due to the seniority mixing for these 1^+ states arising from the influence of the *np* interaction (see below).

The total calculated $B_T(GT)$ strengths in GF, FPG, and GF-GD approaches are 0.11, 0.32, and 2.69, respectively. Clearly, the first two approaches do not agree with the experimental situation as they do not include all of the important transitions. As discussed above, the latter two calculations consist of the GF approach, but also allow additional transitions. In order to obtain a realistic estimate, it is required to retain all the important contributions to the strength and avoid any "double counting" of the transitions. In our calculation, we achieved this by subtracting the GF strength from the sum of the FPG and GF-GD strengths. The experimental value of $B_T(GT) = 1.9\,(5)$ [21] agrees with our calculated value of $0.75^2 \times (2.69 + 0.32 - 0.11) = 1.63$. Here, we have used 0.75 for the quenching factor of the GT operator [39]. The fact that the $B_T(GT)$ value from the GF-GD calculation is much closer to the experimental value emphasizes the strong role of the $\nu g_{7/2}$ orbital. Similar results were also discussed for ^{94,96,98}Pd in Refs. [21,40].

All of the SM calculations have a general feature; namely, they predict small $B(GT)$ strengths into the low-lying states, which are essentially dominated by the $\pi\nu\ g_{9/2}$ orbits and the $\pi g_{9/2} \rightarrow \nu g_{9/2}$ GT transition. This is borne out by the β^+/EC decay data of $N = 48$ isotones [7,21,35]. Even after consideration of the effect from angular momentum re-coupling, the summed strength remains significantly below the extreme single particle estimate (see, e.g., [41]), i.e., $B(GT; \pi g_{9/2} \rightarrow \nu g_{9/2}) = (110/9) n(\pi g_{9/2}) n'(\nu g_{9/2})$, where n and n' are the occupation ratios for $\pi g_{9/2}$ particles and $\nu g_{9/2}$ holes, respectively. This can be understood in terms of the diagonal nature of the odd-tensor part of the GT operator in the seniority scheme [42,43]. The seniority quantum label v is well defined in a pure $g_{9/2}$ model space. Therefore, the calculations in such a space yield negligible GT strengths for the decay of $N = 49$, $v = v_\pi + v_\nu = 1$ (even-odd) and 2 (odd-odd) parent states to their $N = 50$, $v = v_\pi = 3$, 4, and 5 daughter states. This is a clear signature for a seniority conserving interaction. For the low-lying states in nuclei with $N \leqslant 50$, such as those from the present work, an increased seniority mixing is expected due to the influence of the *np* interaction. This could cause a reduction in the GT strength calculated using a seniority conserving interaction. Therefore, our nonobservation of the 1^+ states above 3 MeV in ^{94}Rh due to low values of fragmented $B(GT)$ can be attributed to the effect of the *np* interaction on the low-lying states, especially on the ground state, in ^{94}Pd. It has been argued that such an effect gives rise to the low-lying structure of ^{94}Pd, which is intermediate to that of ^{92}Pd and ^{96}Pd, which have almost equally spaced and seniority type low-lying level schemes, respectively [6].

In Refs. [12,14], the reliability of the evidence found in Ref. [11] for the direct two proton decay of the 21^+ isomeric state in ^{94}Ag was questioned. A hypothetical 2.9-MeV γ ray in ^{94}Rh was used for the arguments in Ref. [14]. Even though a γ ray of 2906 keV is observed in the present work, we would like to stress that a possibility for this γ ray to yield a spurious 1.9-MeV two-proton-like peak in the Si sum spectrum [14] was already discarded in Ref. [44]. At present, neither our observation of the 2906-keV γ ray nor the new data from the mass measurements [13] can exclude the possibility for a two proton decay of the 21^+ isomeric state [11,45–47].

In summary, the low-lying level scheme of ^{94}Rh is deduced by using the observed γ transitions following the ground-state β decay of ^{94}Pd in our experiment. The results are discussed and compared with the shell-model calculations performed in three different approaches. A dominant role of the $g_{7/2}$ orbital is evident and the experimental $B(GT)$ strengths can *only* be explained with its inclusion. The effect of the *np* interaction via seniority mixing on GT hindrance is also discussed for the ground state in ^{94}Pd, which strongly suggests that this nucleus resides in a region exhibiting structural transition. Future experiments designed to enhance the yields for the γ rays following the β decay of ^{94}Pd with respect to that for γ rays from other fragments and theoretical interpretations are suggested to gain further understanding into the structure of the observed 1^+ states. The observed 2906-keV γ ray in our work cannot exclude the possibility of a two proton decay in ^{94}Ag.

This work has been supported by the UK STFC; the German BMBF under Contracts No. 06KY205I, No. 06KY9136I, and No. 06MT9156; the Swedish Research Council; and the DFG Cluster of Excellence, Origin and Structure of the Universe.

[1] H. Grawe *et al.*, Eur. Phys. J. A **27**, 257 (2006).
[2] D. Rudolph, K. R. Lieb, and H. Grawe, Nucl. Phys. A **597**, 298 (1996).
[3] S. Zerguine and P. Van Isacker, Phys. Rev. C **83**, 064313 (2011).
[4] H. Herndl and B. A. Brown, Nucl. Phys. A **627**, 35 (1997).
[5] H. Grawe, *The Euroschool Lectures on Physics with Exotic Beams, Vol. I*, Lecture Notes in Physics Vol. 651 (Springer, Berlin, 2004), p. 33.
[6] B. Cederwall *et al.*, Nature (London) **469**, 68 (2011).
[7] B. S. Nara Singh *et al.*, Phys. Rev. Lett. **107**, 172502 (2011).
[8] P. Woods and C. Davids, Annu. Rev. Nucl. Part. Sci. **47**, 541 (1997).
[9] B. Jonson and G. Nyman, in *Nuclear Decay Modes*, edited by D. N. Poenaru (Institute of Physics, London, 1996), p. 102.
[10] V. I. Goldanskii, JETP Lett. **23**, 554 (1980); Nucl. Phys. **19**, 482 (1960).
[11] I. Mukha *et al.*, Nature (London) **439**, 298 (2006).
[12] O. L. Pechenaya *et al.*, Phys. Rev. C **76**, 011304(R) (2007).
[13] A. Kankainen *et al.*, Phys. Rev. Lett. **101**, 142503 (2008).
[14] D. G. Jenkins, Phys. Rev. C **80**, 054303 (2009).
[15] H. Schatz *et al.*, Phys. Rep. **294**, 167 (1998).
[16] C. Fröhlich *et al.*, Phys. Rev. Lett. **96**, 142502 (2006).

[17] A. Juodagalvis and D. J. Dean, Phys. Rev. C **72**, 024306 (2005).
[18] D. Melconian *et al.*, Phys. Rev. Lett. **107**, 182301 (2011), and the references therein.
[19] K. Oxorn, B. Singh, and S. K. Mark, Z. Phys. A **294**, 389 (1980).
[20] W. Kurcewicz *et al.*, Z. Phys. A **308**, 21 (1982).
[21] L. Batist *et al.*, Eur. Phys. J. A **29**, 175 (2006).
[22] I. P. Johnstone and L. D. Skouras, Phys. Rev. C **53**, 3150 (1996).
[23] D. Abriola and A. A. Sonzogni, Nucl. Data Sheets **107**, 2423 (2006).
[24] G. Audi *et al.*, Nucl. Phys. A **729**, 3 (2003).
[25] T. S. Brock *et al.*, Phys. Rev. C **82**, 061309(R) (2010).
[26] P. Boutachkov *et al.*, Phys. Rev. C **84**, 044311 (2011).
[27] H. Geissel, Nucl. Instrum. Methods B **70**, 286 (1992).
[28] D. Rudolph, Acta Phys. Pol. **42**, 567 (2011).
[29] D. Rudolph *et al.*, Eur. Phys. J. Special Topics **150**, 173 (2007).
[30] H.-J. Wollersheim *et al.*, Nucl. Instrum. Methods A **537**, 637 (2005).
[31] S. Pietri *et al.*, Nucl. Instrum. Methods A **261**, 1079 (2007).
[32] R. Kumar *et al.*, Nucl. Instrum. Methods A **598**, 754 (2009); N. Alkhomashi *et al.*, Phys. Rev. C **80**, 064308 (2009).
[33] Zs. Podolyak *et al.*, Phys. Lett. B **672**, 116 (2009).
[34] S. Pietri *et al.*, Eur. Phys. J. Special Topics **150**, 319 (2007).
[35] http://www.nndc.bnl.gov/ensdf/.
[36] R. Gross and A. Frenkel, Nucl. Phys. A **267**, 85 (1976).
[37] A. Plochocki *et al.*, Z. Phys. A **342**, 43 (1992).
[38] J. C. Hardy *et al.*, Phys. Lett. B **71**, 307 (1977).
[39] E. Caurier *et al.*, Rev. Mod. Phys. **77**, 427 (2005).
[40] K. Rykaczewski *et al.*, Z. Phys. A **322**, 263 (1985) and GSI Report No. 90-62, 1990.
[41] I. S. Towner, Phys. Rep. **155**, 263 (1987).
[42] A. de Shalit and I. Talmi, *Nuclear Shell Theory* (Academic Press, New York, 1963).
[43] R. F. Casten, *Nuclear Structure from a Simple Perspective* (Oxford University Press, Oxford, 2000).
[44] I. Mukha, E. Roeckl, H. Grawe, and S. Tabor, arXiv:1008.5346 [nucl-ex].
[45] I. Mukha, H. Grawe, E. Roeckl, and S. Tabor, Phys. Rev. C **78**, 039803 (2008).
[46] I. Mukha *et al.*, Phys. Rev. Lett. **95**, 022501 (2005).
[47] J. Cerny *et al.*, Phys. Rev. Lett. **103**, 152502 (2009).